ISSN 1674-1056
http://cpb.iphy.ac.cn
http://iopscience.iop.org/cpb
中国物理 B
Chinese Physics
中国物理
Chinese Physics B

An experimental method for quantitative analysis of real contact area based on the total reflection optical principle

Zhijun Luo(罗治军), Baojiang Song(宋保江), Jingyu Han(韩靖宇), Shaoze Yan(阎绍泽)

Citation: Chin. Phys. B . 2019, 28(5): 054601. **doi:** 10.1088/1674-1056/28/5/054601
Journal homepage: http://cpb.iphy.ac.cn; http://iopscience.iop.org/cpb

What follows is a list of articles you may be interested in

Relationship between the real contact area and contact force in pre-sliding regime

Baojiang Song(宋保江), Shaoze Yan(阎绍泽)
Chin. Phys. B . 2017, 26(7): 074601. **doi:** 10.1088/1674-1056/26/7/074601

Image encryption using random sequence generated from generalized information domain

Xia-Yan Zhang(张夏衍), Guo-Ji Zhang(张国基), Xuan Li(李璇), Ya-Zhou Ren(任亚洲), Jie-Hua Wu(伍杰华)
Chin. Phys. B . 2016, 25(5): 054201. **doi:** 10.1088/1674-1056/25/5/054201

Lensless ghost imaging through the strongly scattering medium

Zhe Yang(杨哲), Lianjie Zhao(赵连洁), Xueliang Zhao(赵学亮), Wei Qin(秦伟), Junlin Li(李俊林)
Chin. Phys. B . 2016, 25(2): 024202. **doi:** 10.1088/1674-1056/25/2/024202

Increasing the range accuracy of three-dimensional ghost imaging ladar using optimum slicing number method

Yang Xu, Zhang Yong, Xu Lu, Yang Cheng-Hua, Wang Qiang, Liu Yue-Hao, Zhao Yuan
Chin. Phys. B . 2015, 24(12): 124202. **doi:** 10.1088/1674-1056/24/12/124202

A measurement method for distinguishing the real contact area of rough surfaces of transparent solids using improved Otsu technique

Song Bao-Jiang, Yan Shao-Ze, Xiang Wu-Wei-Kai
Chin. Phys. B . 2015, 24(1): 014601. **doi:** 10.1088/1674-1056/24/1/014601

An experimental method for quantitative analysis of real contact area based on the total reflection optical principle*

Zhijun Luo(罗治军), Baojiang Song(宋保江), Jingyu Han(韩靖宇), and Shaoze Yan(阎绍泽)†

State Key Laboratory of Tribology, Department of Mechanical Engineering, Tsinghua University, Beijing 100084, *China*

(Received 30 November 2018; revised manuscript received 16 January 2019; published online 4 April 2019)

The simulation of real contact area between materials is foundationally important for the contact mechanics of mechanical structures. The Greenwood and Williamson (GW) model and the Majumdar (MB) model are the basic models in this field, which are widely accepted and proven to be valid in many experiments and engineering. Although the contact models have evolved considerably in recent years, the verifications of the models are most based on the indirect methods such as electrical conductivity and contact stiffness, because of the lack of effective methods to directly measure the variation of contact surface. In this paper, the total reflection (TR) method is introduced into the verification of contact models. An experiment system based on TR method is constructed to measure the real contact area of two PMMA specimens. The comparison analysis between the results of experiment and models suggests that the experiment result has the same trend with simulation, the MB model has better agreement with the experimental result because this method can take into account the variation of radius and the merging of asperities, while the GW model has a huge deviation because of the dependence on resolution and the lack of considering the variation of radius and asperity's merging process. Taking the interaction of asperities into account could give a better result that is closer to the experiment. Our results and analysis prove that the experimental methods in this paper could be used as a more direct and valid method to quantitatively measure the real contact area and to verify the contact models.

Keywords: real contact area, Greenwood and Williamson (GW) model, Majumdar (MB) model, Persson's model, total reflection (TR) method

PACS: 46.55.+d, 42.30.Va, 78.20.Ci **DOI:** 10.1088/1674-1056/28/5/054601

1. Introduction

A model of the real contact area between materials is foundationally important for the friction, sliding, seals, wear, structure stiffness and damping, thermal and electrical conductivity, and other aspects of engineering.[1–3] This subject has attracted interest of researchers for over 500 years. In 1495, when Leonardo da Vinci first found the fundamental laws of friction by experimenting with ball-bearings, revealing that the frictional force is independent of the contact surfaces.[1] In 1699, Amontons rediscovered the laws of friction and in 1781 Coulomb enriched and systematically summarized the laws.[1] The recently most important contribution was made by Bowden and Tabor in 1939, who found that the real contact area between two materials consists of a myriad of contact asperities, and is orders of magnitude smaller than the nominal contact area.[4] Based on this theory, in 1966 Greenwood and Williamson (GW) proposed the pioneering GW model, which simulates the real contact area by integrating the contact area of single asperity under normal pressure, assuming that the height of asperities varies randomly comply with the Gaussian distribution, every asperity summit has the same curvature radius, the asperities are independent of each other, and the deformation is mainly elastic. Despite the crudeness of the GW model, it has been widely applied and validated by many experiments, and leaded to many derivative models, such as the WA model proposed by Whitehouse and Archard (WA) in 1969 by considering the distribution of asperity curvature,[6] the OA model proposed by Onions and Archard (OA) in 1972 by utilizing the WA model to determine the relationship between the separation and contact area,[7] and many other models considering new factors for the special problems.[8,9] However, many of the parameters of these models are determined by the resolution of apparatus, such as roughness and profile of surface, which will cause the un-uniqueness of the results. In 1991, Majumdar argued that the mechanic surface has self-affine fractal characteristics, and proposed the contact fractal theory and the corresponding MB contact model, in which the major parameters fractal dimension D and characteristic length scale G are scale invariance. This characteristic will guarantee the uniqueness of results.[10] The MB model also has been widely applied to structure stiffness and damping simulation and proved to be valid in the prediction of stiffness and damping of the mechanic contact surface.[11,12] Despite the different interpretation for contact surface, GW model and MB model both have many supporters, and in recent years some new more accurate models have been proposed by researchers based on these two models. For example, the Zhao, Maietta, and Chang (ZMC) model is based on

*Project supported by the National Natural Science Foundation of China (Grant No. 11872033) and the Beijing Natural Science Foundation, China (Grant No. 3172017).

†Corresponding author. E-mail: yansz@mail.tsinghua.edu.cn

© 2019 Chinese Physical Society and IOP Publishing Ltd

the GW model considering the transition from elastic deformation to fully plastic flow,[13] the Kogut and Etsion (KE) model also based on GW model considers the interaction of neighboring asperities,[14] Persson's model inheriting from multi-scale principle of MB model can take the interaction into account from the special physical view of contact diffusion,[23–25] and the newest paper[15] considered the interaction of asperities based on the MB model.

Although the contact models have evolved considerably, the verifications of these models are most based on the indirect methods, such as electrical conductivity and contact stiffness.[11–15] Whereas, directly observing the real contact area between two bodies should be a more accurate experimental method to measure the variation of the contact surface under different load, and to verify the contact models. Along with the improvements in the technique, researchers have recently tried to directly observe the contact surface using advanced techniques. For example, Eguchi analyzed the interface distribution of the contact area by using white light interference.[16] Tuononen used a high-speed camera to record the contact area of interface between rubber sample and the glass surface.[17] However, these methods can only measure the contact interface between the transparent material and non-transparent material. Kim presented a method that can predict the real contact area between solids by utilizing the data from ultrasonic measurement.[18] Bettscheider proposed a foot-printing approach to determine the real contact area by measuring the foot-printing on a thin marker layer on the interface.[19] However, these methods are a little complicated and hard to realize. Rubinstein, in 2004, proposed a total reflection (TR) method to observe the real contact surface, which is based on the optical theory that the light only passes through the contact asperities between two transparent materials when the angle of incidence is greater than the critical angle.[20] The TR method has been proven to be easy to implement, and effective in the observation of real contact area between two transparent materials, which are testified by some breakthrough discoveries based on this method.[21]

In this paper, an experiment system based on TR method is constructed to measure the real contact area of two polymethyl methacrylate (PMMA) specimens, the variation of real contact area under normal force is quantitatively studied by experiment and simulation using GW model and MB model.

The rest of this paper is organized as follows. Section 1 briefly introduces the principle of GW model and MB model. Section 2 introduces the constructed experimental system. Section 3 implements the comparison analysis for the results between the experiment and models. Section 4 concludes the study.

2. The GW model and MB model

Although some new revised formulas in recent years have been proposed to calculate the real contact area and related stiffness and damping of contact surface,[13–15] the principle can almost all stem from the two basic models: GW model and MB model. In this section, these two basic models will be introduced and analyzed. Because the definition about real contact area has different meaning in different research scale.[29–31] To avoid ambiguity, we defined here that real contact area means the area having true contact between two surfaces, and nominal contact area means the shape of the surface which appears to contact.

2.1. GW model

Since Bowden and Tabor in 1939 found that the real contact area between two materials consists of a myriad of contact asperities,[4] how to determine the deformation of asperities and how to calculate the distribution and the variation of asperities have attracted much interest. The Hertz contact theory is classical and widely accepted for the elastic deformation of sphere contact, and is generally used to calculate the elastic deformation of asperities.[5] As shown in Fig. 1, each peak of asperity is deemed to be a sphere with a radius R, the contact of two asperities can be equivalent to an asperity contacting with a rigid plane, the equivalent parameters can be obtained by

$$\frac{1}{E} = \frac{1-\upsilon_1^2}{E_1} + \frac{1-\upsilon_2^2}{E_2}, \tag{1}$$

$$\frac{1}{R} = \frac{1}{R_1} + \frac{1}{R_2}, \tag{2}$$

the relationships between deformation δ and contact area A_a and between δ and normal force P_a can be respectively obtained as

$$A_a = \pi R\delta, \tag{3}$$

$$P_a = \frac{4}{3}ER^{1/2}\delta^{3/2}, \tag{4}$$

where E is the equivalent elastic modules, and R is the equivalent radius.

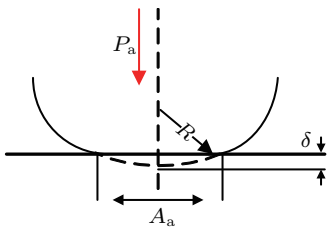


Fig. 1. The deformation of sphere and flat rigid plane, R is the radius of asperity, δ is the normal deformation, A_a is the area of deformation, and P_a is the normal force.

Based on this contact theory, and considering that the deformation of asperities is major elastic, in 1966, Greenwood

and Williamson proposed the GW model, which assumed that the height distribution of peaks of asperity is Gaussian, the radii of peaks all equal to the mean radius of curvature, and the asperities are all independent of each other. On the basis of these assumptions, a simple relationship about normal force and real contact area can be obtained, as shown in Fig. 2. The mean height of asperities is used as a reference plane, the separation of rigid plane and reference plane is d, then the deformation can be obtained by

$$\delta = z - d, \tag{5}$$

where the height distribution of a peak is $\phi(z)$.

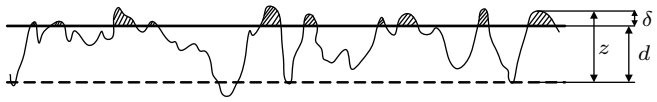


Fig. 2. A schematic of the contact surface: the dashed line is the reference plane which is the average line of the height of asperities, the solid line represents the rigid plane, the curve is the profile of surface, and the shadow areas are the real contact area, or named deformation of asperities.

The probability of an asperity having real contact area $A_a = \pi R\delta$ is the integration from d to infinity of the normal distribution function multiplied with the contact area, which can be written as

$$A_a = \pi R \int_d^\infty (z-d)\phi(z)\mathrm{d}z, \tag{6}$$

where $\phi(z)$ is the normal distribution function

$$\phi(z) = \frac{1}{\sigma\sqrt{2\pi}} \mathrm{e}^{-z^2/2\sigma^2}, \tag{7}$$

with σ being the variance of the height of asperities.

Therefore, the total real contact area can be acquired by summing the possible contact areas of all asperities as

$$A_r = A\eta A_a = A\eta\pi R \int_d^\infty (z-d)\phi(z)\mathrm{d}z, \tag{8}$$

where A_r is the total real contact area, A is the nominal contact area, η is the density of asperities, $A\eta$ is the number of asperities, z is the height of asperity, and d is the distance between the rigid plane and reference plane of surface.

Following this method, the total normal force can be obtained by

$$P_r = \frac{4}{3} A\eta E R^{1/2} \int_d^\infty (z-d)^{3/2}\phi(z)\mathrm{d}z. \tag{9}$$

2.2. MB model

Although the GW model is simple and proven to be valid in many contact cases,[5–9] the accurate parameters such as height, radius, density, and variation of height are determined by the resolution of measurement apparatuses and hard to be obtained. For example, the density of asperity is difficult to be determined if the asperities have no obvious separation line, and will change with the resolution. In 1999, Majumdar argued that although the topography of surface will change with the resolution of measurement, the topography in different scale is self-affine which is similar to the self-similar of topography of earth surface. Based on this discovery, they introduced the fractal theory into contact surface and developed the MB model.[10]

The MB model uses two major parameters to depict the topography of an asperity: the fractal dimension D and the characteristic length scale G, which can be used to express the profile of a surface by utilizing Weierstrass–Mandelbort (WM) function

$$z(x) = G^{(D-1)} \sum_{n=n_1}^{\infty} \frac{\cos(2\pi\gamma^n x)}{\gamma^{(2-D)n}}, \quad 1 < D < 2, \quad \gamma > 1, \tag{10}$$

where γ^n determines the frequency spectrum of the surface roughness, and the lowest frequency is determined by the length of the sample as $\gamma^{n_1} = 1/L$.

When thinking about the profile of a single asperity, which has a contact length $l = \sqrt{A_a}$, formula (10) can be approximated as

$$z(x) = G^{(D-1)} l^{(2-D)} \cos\left(\frac{\pi x}{l}\right), \quad -\frac{l}{2} < x < \frac{l}{2}, \tag{11}$$

where x is the length of surface profile of an asperity, which for a single asperity is in the range of length l, and z is the height of an asperity at the position x.

Because the position $x = 0$ can be deemed as the center point of an asperity, then the radius of a single asperity can be obtained by

$$R = 1 \Big/ \left|\frac{\mathrm{d}^2 z}{\mathrm{d}x^2}\right|_{x=0} = \frac{A_a^{D/2}}{\pi^2 G^{(D-1)}}, \tag{12}$$

where the radius is not constant and will vary with the real contact area. And the deformation in the center point can be given by

$$\delta = z(0) = G^{(D-1)} A_a^{(2-D)/2}. \tag{13}$$

So the related normal force acting on an asperity can be expressed as

$$P_a = \frac{4}{3}\sqrt{\pi} E G^{(D-1)} A_a^{(3-D)/2}. \tag{14}$$

If the surface of material is zoomed enough, the asperities will appear similar with the earth's hills and valleys, and the horizontal cross-section of asperities would be analogous to the section of islands horizontally cut by ocean. The law for the number of islands has been found by Mandelbrot in 1975, which is expressed as

$$N(A > a) = a^{(-D/2)}, \tag{15}$$

where N is the number of islands with the area larger than a, and D is the fractal dimension.

In the MB model, the size distribution of contact asperities is deemed to be the same with the distribution of the islands on earth. When normalizing Eq. (14) with the largest contact spot A_l, the number of asperities can be expressed as

$$N(A > A_a) = \left(\frac{A_l}{A_a}\right)^{D/2}, \tag{16}$$

where A_l is the largest contact area of an asperity, and N is the number of asperities with the area bigger than A_a.

Therefore, the distribution density can be obtained by the differentiation of Eq. (16) as

$$n(A_a) = \left|\frac{dN}{da}\right| = \frac{dA_l^{D/2}}{2A_a^{(D/2+1)}}. \tag{17}$$

When integrating the contact area and normal force in the total nominal surface, combining with formula (14), the formulas for the real contact area and normal force can be expressed as

$$A_r = \int_0^{A_l} n(A_a)A_a dA_a, \tag{18}$$

$$P_r = \frac{4\sqrt{\pi}EG^{D-1}}{3}\int_0^{A_l} n(A_a)A_a^{(3-D)/2}dA_a, \tag{19}$$

where A_r is the real contact area of surface under normal force P_r.

2.3. The plastic deformation

Actually, the deformation will become plastic when the deformation of asperity increases beyond the critical value δ_c given by[10]

$$\delta_c = \left(\frac{\pi H}{2E}\right)^2 R, \tag{20}$$

where H is the hardness, E is the Young's modulus, and R is the radius of asperity.

In the MB model, R is determined by Eq. (12), and δ_c has the form

$$\delta_c = \left(\frac{H}{2E}\right)^2 \frac{A_a^{D/2}}{G^{(D-1)}}. \tag{21}$$

In plastic deformation, the normal pressure supported by asperity is constant, and is equal to the hardness, therefore, the normal force of plastic deformation can be expressed as

$$P_{ap} = H \cdot A_a. \tag{22}$$

When taking the plastic deformation into account, the formulas for the GW model should be changed to

$$\begin{aligned} A_r &= A_e + A_p \\ &= A\eta\pi R\left(\int_d^{d+\delta_c}(z-d)\phi(z)dz + \int_{d+\delta_c}^{\infty}(z-d)\phi(z)dz\right), \\ P_r &= P_e + P_p = \frac{4}{3}A\eta E R^{1/2}\int_d^{d+\delta_c}(z-d)^{3/2}\phi(z)dz \\ &\quad + A\eta\pi R\int_{d+\delta_c}^{\infty}(z-d)\phi(z)dz, \end{aligned} \tag{23, 24}$$

where A_e is the elastic contact area, A_p is the plastic contact area, P_e is the normal force supported by the elastic contact area, and P_p is the normal force supported by the plastic contact area.

Likewise, for the MB model, the critical value of contact area A_c can be derived out by combining Eqs. (12), (13), and (21) as

$$A_c = \frac{G^2}{(H/2E)^{(2/(D-1))}}. \tag{25}$$

The formulas for the MB model can be changed to

$$\begin{aligned} A_r &= A_e + A_p \\ &= \int_0^{A_c} n(A_a)A_a dA_a + \int_{A_c}^{A_l} n(A_a)A_a dA_a, \end{aligned} \tag{26}$$

$$\begin{aligned} P_r &= P_e + P_p \\ &= \frac{4\sqrt{\pi}EG^{D-1}}{3}\int_0^{A_c} n(A_a)A_a^{(3-D)/2}dA_a + H\int_{A_c}^{A_l} n(A_a)A_a dA_a. \end{aligned} \tag{27}$$

When dividing Eq. (21) by Eq. (13), the relationship of deformation and critical deformation can be expressed as

$$\frac{\delta_c}{\delta} = \left(\frac{A_a}{A_c}\right)^{(D-1)}, \tag{28}$$

where the ratio between the critical deformation and deformation is reverse to the ratio of the critical contact area and contact area.

Analyzing Eq. (28), we should notice that when $\delta > \delta_c$, for the MB model, $A_a < A_c$, while for the GW model, $A_a > A_c$, vice versa. This means that the plastic judgment in GW is just opposite to that in MB model when using contact area as criteria. In the GW model, when the contact area is larger than the critical value, the deformation obviously is plastic; while in MB model, it is elastic, and vice versa.[5,10] This is one of the major differences between the GW and MB models. The physical reality is that the pressure will be very big when the contact peak is very small, so the deformation is plastic, when the radius becomes large caused by the deformation, the pressure will become small, and the deformation is elastic. From this angle, the MB model considering the change of radius is more reasonable. However, the GW model also suggests that the deformation will remain elastic because new contact peaks will join to support the load instantly to lead the deformation stay in elastic when the contact peak is small. More details and formulas can be obtained from the references.[5,10]

Despite the different interpretation, the GW model and MB model both obtain many supports from researchers and are proven to be valid in many cases calculating the stiffness and

damping.[14,15] However, neither stiffness nor damping is a direct indicator to verify the formula, while measuring the real contact area would give a more direct experimental measurement for these formulas. In the next sections, an experiment setup is constructed to measure the real contact area based on the TR method, and the qualitative comparison analysis between simulation and experiment will be implemented.

3. The experiment of the real contact area

The beam transmitting from a denser medium to a thinner one will be totally reflected back into the denser medium when the incident angle is greater than the critical angle.[20] As shown in Fig. 3, when pressing two transparent blocks together, the contact surface is formed by many contacted asperities, between which are gaps full of air. The beam beyond critical angel will only be reflected by the gaps and transmits out at the contacted asperities. Naturally, the intensity of the transmitting beam corresponds to the real contact area.

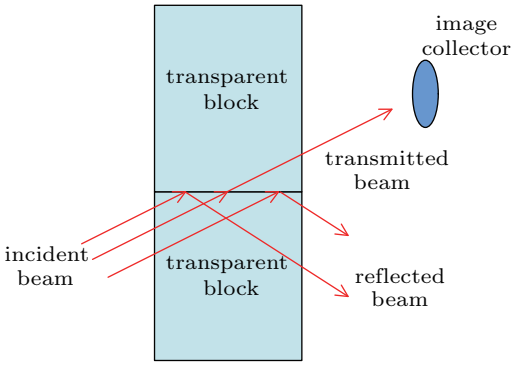


Fig. 3. Schematic of the TR method.

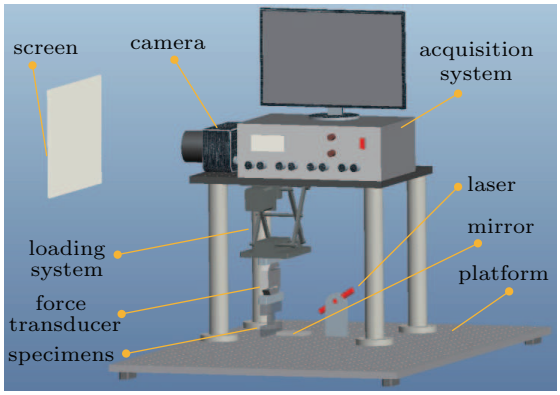


Fig. 4. A 3D diagram of experiment system.

Based on this principle, we build an experiment setup to measure the contact area under normal force. As shown in Fig. 4, the normal force is produced by an X type lifting device driven by a stepper motor with a screw, a laser beam reflected by a mirror transmits the PMMA block and images on the screen, a camera is used to record the image, and a data acquisition device is used to record the normal force. The field photo is shown in Fig. 5. The parameters of the major devices and PMMA are listed in Table 1.

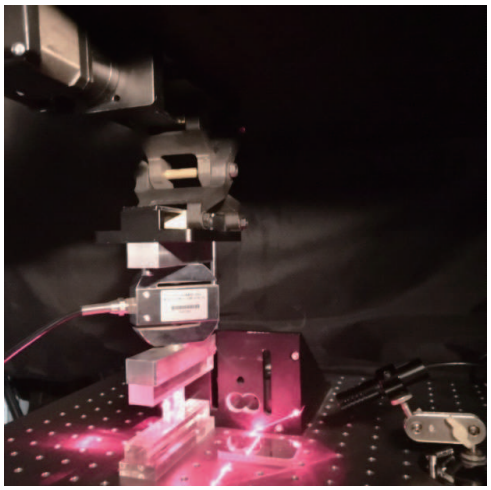


Fig. 5. The field photo of experiment system.

Table 1. Parameters of major devices and material.

Device	Style	Parameters
Laser	semiconductor	650 nm
Camera	NIKON D610	CMOS: 24.26M pixels
Stepper motor	400	maximum force 1 kN
Force transducer	S type	0–500 N
Acquisition device	INV306U	16 bit
Specimen	PMMA block	20 mm×10 mm×20 mm

The experiment is carried out, the camera is set to manual mode at ISO 2200 and f 4.0, the sampling rate of normal force is 1024 with low-pass filtering at 30 Hz. To ensure that the surface is enough flat and transparent, the nature surface of PMMA block without other polishing is utilized as the experimental surface. The normal load increases at constant speed and stops at every test point. To avoid the creep of PMMA, we only take three photos at every test point to obtain the average greyscale in very short time interval, about several seconds. The recorded images are shown in Fig. 6. Figure 6(a) shows the images under different normal force, where the red area and brightness grow up with the normal force. Figure 6(b) shows the normal curve of force and real contact area, the coordinate is normalized by the ratio between the real contact area and nominal contact area, the nominal contact area A is calculated by the intensity of laser directly transmitting to the screen without obstruction of the PMMA block. Because the laser is red, so the intensity is obtained by integration of the grayscale of red color as expressed by

$$A_{\mathrm{k}} = \sum_{i}^{m}\sum_{j}^{n} R_{\mathrm{k}}(i,j), \tag{29}$$

where R_{k} is the red grayscale of a pixel.

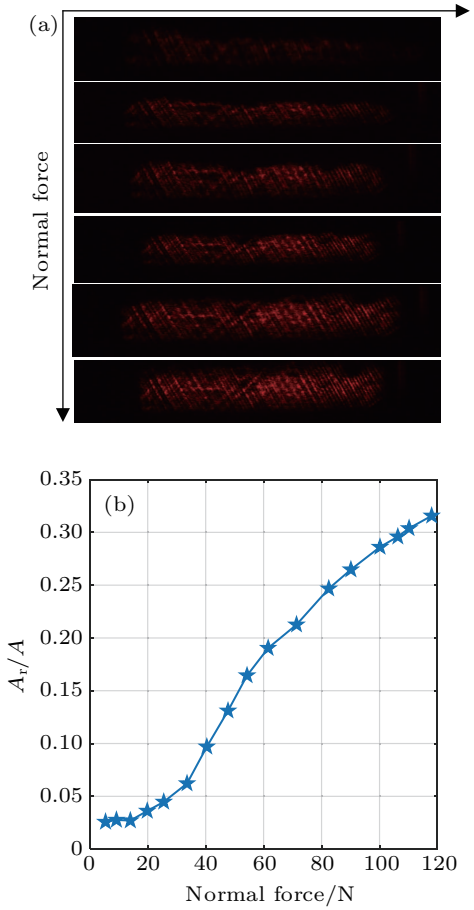


Fig. 6. The results of experiment: (a) the images under different normal force, where the red area and brightness grow up with the normal force, (b) the curve of normal force and real contact area, the force has been scaled to the nominal contact area considering the whole surface is larger than the recorded nominal contact area.

4. Simulation and comparison

In this section, the surface topography is scanned by the white light interferometer, and the surface parameters used to calculate the real contact area are calculated based on the obtained image, the curve of normal force and real contact area obtained from GW model, MB model, and experiment are plotted in a graph to comparatively analyze the results.

4.1. Parameters calculation

The white light interferometer shown in Fig. 7 is used to measure the experimental surface with area 834.370 μm×834.370 μm, and the image of topography is shown in Fig. 8, where the surface is flat and has a small variation. The height distribution of peaks is shown in Fig. 9, where the distribution is approximate Gaussian. The curvature radius of peaks is calculated at the X and Y directions respectively, the mean radius of all peaks in the two directions is used as the radius for the GW model.

For the MB mode, the parameters D and G can be obtained from the power spectrum of profile of surface, which can be expressed as

$$F(\omega) = \frac{G^{2(D-1)}}{2\ln\gamma\omega^{(5-2D)}}, \tag{30}$$

where $F(\omega)$ is the power spectrum, and γ is usually set to 1.5.



Fig. 7. The photo of white light interferometer made by Z YGO company, having 0.1 nm resolution.

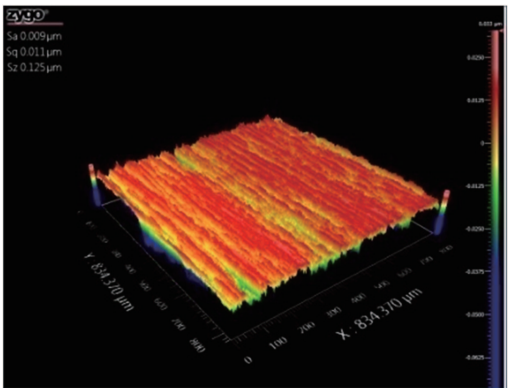


Fig. 8. The surface topography of the specimen.

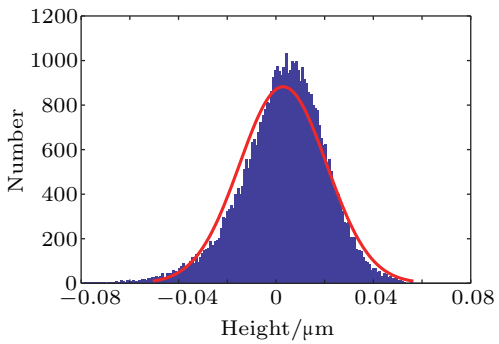


Fig. 9. The distribution of height of peaks, the zero point is the mean value.

In the log–log coordinate, the curve of ω and $F(\omega)$ is an approximate straight line. If the slope is in the range of -3 to -1, the surface is deemed to be fractal, and D and G can be calculated using the slope and intercept of line as

$$D = (k+5)/2, \tag{31}$$

$$G = 10^{(b+\log(2\ln\gamma)/2(D-1))}. \tag{32}$$

First, the power spectrum of every column and row of image is calculated by using Fourier transform, the mean value of the power spectrum is used to map on the log–log coordinate, and the fitting line is then obtained by the least square method. The fitting line and power spectrum are shown in Fig. 10.

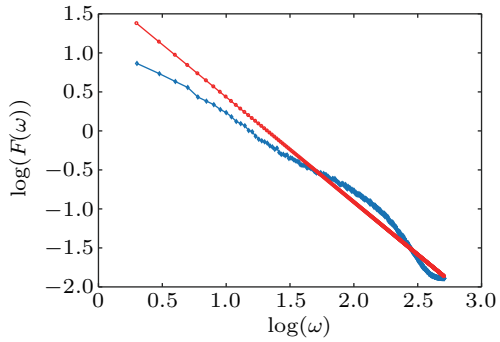


Fig. 10. The power spectrum and the fitting line of surface topography.

The resulting parameters for the two models and the characteristic parameters of material are listed in Table 2. In the table, the radius is very large because the surface is very flat and has strips cluster area which also can be seen in Figs. 5 and 6, the density of asperities is determined by the number of local peaks counted by a computer program, the nominal contact area is determined by the width of laser transmitting the specimen, because only in these range the real contact area can be observed.

Table 2. Parameters of models and material.

Parameters	GW	MB
Mean radius R	781.87 μm	–
Density of asperity η	6.608×10^4 mm^{-2}	–
Variation of asperity σ	0.00178 μm	–
Fractal dimension D	–	1.8165
Characteristic length scale G	–	6.807×10^{-12}
Young modulus E	532 MPa	
Poison's rate υ	0.4	
Hardness H	150 MPa	
Nominal contact area A	19.31×4.0 mm^2	

4.2. Comparison analysis

The parameters are substituted into the models, and the results of experiment and simulation are plotted in Fig. 11. In the figure, the contact areas of GW and MB linearly increase with the growth of normal force, the experimental result appears the similar trend with the simulation. In the initial part of the experimental result, the line is almost horizontal because the load is very small, the contact spots are too small to let the light pass though. When the load increases after the initial part, the real contact area increases linearly and has a good agreement with the MB model but has an obvious big deviation from the GW model. As the load increases much more, the deviation to the MB model also gradually becomes bigger.

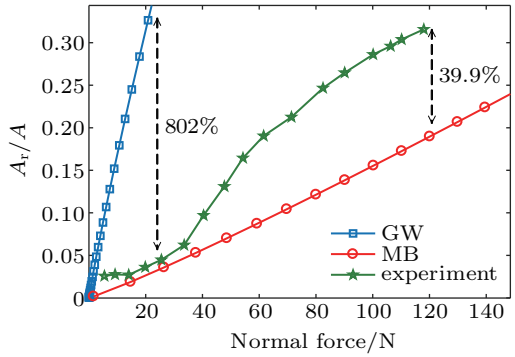


Fig. 11. The normal force and ratio of real contact area to the nominal contact area.

At small load, deformation is small and the asperity is well separated, so the GW and MB models would have a good prediction, this is generally accepted and verified by many researchers. For example, Hyun proved that the relationship of real contact area and load is linear when the fraction of contact area is smaller than 0.1,[22] our experimental result also agrees with this. Although Persson had a different opinion for the contact model, he also admitted that the GW model and MB model are accurate at small load.[23]

What causes the big deviation to the GW model in the small load region? We can obtain two explanations from the paper about MB model.[10] One is that the parameters of GW model will be greatly affected by the resolution of measurement devices. The white interferometer used in this experiment has the resolution of 0.1 nm, which is significant higher than that of the experiment finished in the past time. Persson also argued that GW model just considers one scale of the surface which is not very accordance with the reality;[23] i.e., the resolution for GW model should be in a matched scale. Another explanation is that the GW assumes a constant radius, which is not consistent with the reality and also the phenomena in our experiment where strip cluster is obvious even in small load area. In contrast, the MB model takes into account the change of radius and the merging of neighboring asperities, which is more reasonable at least for this experiment where the asperities emerging phenomenon is also evident as shown in Fig. 5.

It also can be noticed that MB model has an increasing deviation to the experiment result. Persson thought that GW and MB both lack the ability to model the interaction of asperities,[23–25] which will greatly affect the result at heavy load. Some other researchers also pointed out this problem and proposed revised models. For example, Zhao derived the revised method by utilizing the Saint–Vansant's principle and proved that the revised model has a larger contact area than the original GW model under the same load.[13] Tang proposed a numerical iterative method to model the interaction of the asperities, and showed that in the revised mode, the deformation of asperities would be larger than that in the original model

which is based on GW model.[28] Likewise, following this revised method, if the interaction is taken into account in the MB model, then the curve would be more close to the experiment result. Persson also proposed a new multi-scale model from different physical angle,[23,24] which derived an equation similar to the diffusion function to depict the process of real contact area changing with scale and load, and argued that it can take into account the elastic coupling between asperities and is more accurate than the GW and MB models.[24] A problem should be noticed that the MB model takes every scale of surface into account; however, it can be observed in the color images of Fig. 5 that the black strip area exists in the whole process, which means that some area maybe never have contact, i.e., the contact may not occur in some large scale. Persson deemed that there is a cut off length for the contact.[23] Following this theory, the nominal contact area would be smaller, and the fraction of contact area will be bigger to make the result of MB model closer to the experiment. However, Persson's model is still questioned by some researchers and needed more researches.[26,27] Considering that interaction of asperities is a complicated problem, in this paper we do not discuss this point further but focus instead on the experimental method and the verification of the two basic models.

From the results and analysis, it can be concluded that the total reflection method and the related experimental method in this paper would be valid to be used as a quantitative method for the real contact area measurement. Based on this direct measurement method, the researcher not only can analyze the evolution of interface under different load and condition but can also compare and verify many revised contact models and newly developed contact models. This experimental method has foundational value for research of contact mechanisms and the related interface character.

5. Conclusion

The direct observation method for real contact area, TR method, is used to quantitatively verify the original GW model and MB model. The experiment system based on TR method is constructed to measure the real contact area of two PMMA specimens, the curves of real contact area and normal force obtained by the experiment and models are plotted in the same coordinate, the comparison analysis suggests that the MB model has better agreement with the experimental result because this method can take into account the variation of radius and the merging of asperities, while the GW model has a huge deviation because of the dependent on resolution and the lack of consideration of the variation of radius and asperity's merging process. If we take the interaction of asperities into account, then the results of models would have better agreement with the experiment. The results and analysis prove that the experimental methods in this paper could be used as a more direct and valid method to quantitatively measure the real contact area and to verify the contact models. This experimental method has the foundational value for research of contact mechanisms and the related interface character.

References

[1] Popov V L 2010 *Contact Mechanics and Friction* (Heidelberg Berlin: Springer) p. 5
[2] Song B J and Yan S Z 2017 *Chin. Phys. B* **26** 074601
[3] Song B J, Yan S Z and Xiang W K 2015 *Chin. Phys. B* **24** 014601
[4] Bowden F P and Tabor D 1939 *Proc. R. Soc. London* **169** 391
[5] Greenwood J A and Williamson J B P P 1966 *Proc. R. Soc.* **295** 20539169
[6] Whitehouse D J and Archard J F 1970 *Proc. R. Soc. London* **316** 97
[7] Onions R A and Archard J F 1973 *J. Phys. D Appl. Phys.* **6** 289
[8] Chang W R, ETSION and IBOGY D B 1987 *J. Tribol.* **109** 257
[9] Horng J H 1998 *J. Tribol.* **120** 82
[10] Majumdar A and Bhushan B 1991 *J. Tribol.* **113** 1
[11] Zhang X L 2002 *Trans. Chin. Soc. Agricultural Machinery* **33** 91
[12] Jiang S Y, Zheng Y J and Zhu H 2010 *J. Tribol.* **132** 011411
[13] Zhao Y Z and Chang L 2001 *J. Tribol.* **123** 857
[14] Sepehri A and Farhang K A 2011 *Modell. Simul. Eng.* **46** 383
[15] Wang R Q, Zhu L D and Zhu C X 2018 *J. Mechanical Engineering* **54** 88 (in Chinese)
[16] Eguchi M, Shibamiva T and Yamamoto T 2009 *Tribol. Int.* **42** 1781
[17] Tuonoen A J 2014 *Tribol. Int.* **69** 70
[18] Kim J Y, Baltazar A and S I 2004 *Rokhlin J. Mech. & Phys. Solids* **52** 1911
[19] Bettscheider S, Gachot C and Rosenkranz A 2016 *Tribol. Int.* **103** 167
[20] Rubinstein S M, Cohen G and Fineberg J 2004 *Nature* **430** 1005
[21] David B, Rubinstein S M and Fineberg J 2010 *Nature* **463** 76
[22] Hyun S, Pei L and Molinari J F 2004 *Phys. Rev. E Stat. Nonlin. Soft Matter Phys.* **70** 026117
[23] Persson B N J 2006 *Surf. Sci. Rep.* **61** 201
[24] Persson B N J 2001 *J. Chem. Phys.* **115** 3840
[25] Persson B N J 2001 *Phys. Rev. Lett.* **87** 116101
[26] Manners W and Greenwood J A 2006 *Wear* **261** 600
[27] Yastrebov V A, Anciaux G and Molinari J F 2014 *Tribol. Lett.* **56** 171
[28] Tang Z C, Jiao Y Y and Wong L N Y 2017 *Int. J. Rock Mech. Min. Sci.* **97** 15
[29] Mo Y, Turner K T and Szlufarska I 2009 *Nature* **457** 1116
[30] Liu Z 2014 *Nanotechnology* **25** 075703
[31] Sun J, Zhang Y and Lu Z 2018 *J. Phys. Chem. Lett.* **9** 2554